01 Aug 2004

Expert System Algorithms for Identifying Radiated Emission Problems in Printed Circuit Boards

Hwan-Woo Shim

Todd H. Hubing
Missouri University of Science and Technology

Thomas Van Doren
Missouri University of Science and Technology, vandoren@mst.edu

Richard E. DuBroff
Missouri University of Science and Technology, red@mst.edu

et. al. For a complete list of authors, see https://scholarsmine.mst.edu/ele_comeng_facwork/1615

Recommended Citation

H. Shim et al., "Expert System Algorithms for Identifying Radiated Emission Problems in Printed Circuit Boards," *Proceedings of the IEEE International Symposium on Electromagnetic Compatibility (2004, Santa Clara, CA)*, vol. 1, pp. 57-62, Institute of Electrical and Electronics Engineers (IEEE), Aug 2004.
The definitive version is available at https://doi.org/10.1109/ISEMC.2004.1349996

Expert System Algorithms for Identifying Radiated Emission Problems in Printed Circuit Boards

Hwan Shim, Todd Hubing, T. Van Doren, R. DuBroff, J. Drewniak and D. Pommerenke
Electromagnetic Compatibility Laboratory
University of Missouri-Rolla
Rolla, MO, USA

Robert Kaires
Mentor Graphics Corporation
Wilsonville, OR, USA
robert_kaires@mentorg.com

Abstract—**Radiated emission algorithms for a printed circuit board EMC expert system are described. The expert system mimics the thinking processes that human EMC engineers would use to analyze circuit boards and make design recommendations. Working with limited information about the enclosure, cables or the exact nature of the signals, the expert system evaluates different structures on the printed circuit board looking for potentially strong radiated emission sources. Results obtained from the analysis of a sample printed circuit board are provided to demonstrate how the expert system quickly identifies problems that would otherwise be difficult to locate.**

Keywords-EMC; Expert system; current-driven radiation; voltage-driven radiation

I. INTRODUCTION

Although there are many computer modeling tools on the market these days, EMC engineers rarely use them to analyze printed circuit board (PCB) layouts. Computer modeling can provide valuable insight to a board designer as critical circuits are being placed and routed, but they are not very good at identifying the unintentional emissions sources and coupling paths that result in most EMC problems. Full-wave modeling of printed circuit boards is not a practical option considering the complexity of today's electronic devices. Even with infinite computational resources, the board designer would not normally have all the necessary information about the components, signals and software necessary to do an accurate analysis. Furthermore, EMI test procedures have repeatability issues that prevent their results from being accurately predicted by computer models [1].

Despite the lack of information necessary to do full-wave modeling, experienced human EMC engineers are generally able to identify potential EMC problems in a printed circuit board layout and estimate the impact that these problems will have on system emissions. Expert system approaches attempt to emulate the processes used by human EMC engineers to allow printed circuit board designers to identify potential problems earlier in the design process [2]-[7].

The PCB EMC expert system algorithms developed at the University of Missouri-Rolla consist of four stages as described in [3]. The basic structure is shown Fig. 1. Using board layout and component input data, the characteristics of all the nets and their signals are identified in the net classification stage. This information is passed to the evaluation algorithms, which search for possible radiation or susceptibility problems. In this paper, the radiation algorithms in the evaluation stage are described. There are four different radiation algorithms: the *Differential-Mode Radiation* algorithm, the *Current-Driven Common-Mode Radiation* algorithm, the *Voltage-Driven Radiation* algorithm, and the *Radiation by I/O Coupling* algorithm. The *Differential-Mode Radiation* algorithm calculates the direct radiation from signal traces (which is usually negligible in well designed boards). The *Current-Driven Common-Mode Radiation* algorithm determines how well each circuit is able to drive common-mode currents onto the cables or enclosure by way of magnetic field coupling. The *Voltage-Driven Radiation* algorithm focuses on electric field coupling. Finally, the radiation due to noise coupled directly to traces that conduct energy off the board is calculated by the *Radiation by I/O Coupling* algorithm.

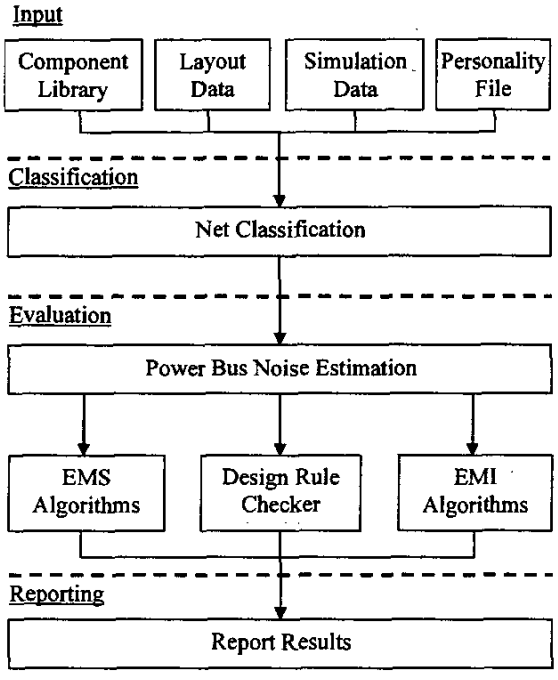

Fig. 1. Structure of the PCB EMC expert system.

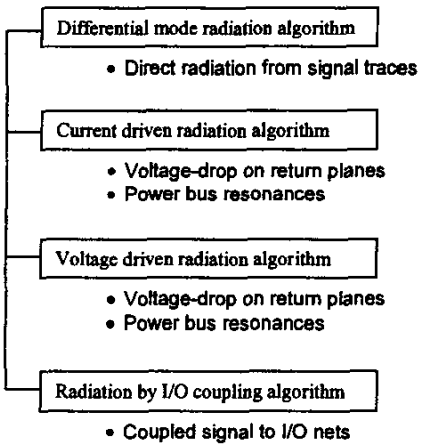

Fig. 2. Radiated emission algorithms.

II. RADIATION ALGORITHMS

The radiated emissions algorithms are listed in Fig. 2 along with their primary subroutines. The following sections summarize the basic operation of these algorithms.

A. Differential-Mode Radiation Algorithm

This algorithm models signal trace segments and their corresponding return trace segments as current loop radiation sources. The maximum electric field is given as [8]

$$|E|_{max} = 1.316\times10^{-14}\left.\frac{|I_D|\ f^2 l\ s}{r}\right|_{r=3m} \approx 4.4\times10^{-15}\ |I_D|\ f^2 l\ s \tag{1}$$

where, f is frequency (in Hz), l is the length of a segment and s is the distance between trace and return trace (or twice the spacing between the trace and the closest return plane). I_D is the magnitude of the signal current. Since most EMI regulations require measurements in a semi-anechoic environment, the field is multiplied by a factor of two to account for the worse-case reflection off the floor,

$$|E|_{max} = 4.4\times10^{-15}|I_D|\ f^2\ l\ s\times2 \approx 10^{-14}|I_D|\ f^2\ l\ s \tag{2}$$

Each segment of every net on the board is evaluated by this algorithm at each frequency of interest. The differential emission estimate for the entire board is obtained by taking a root mean square sum of the fields for each net as

$$|E|_{total} = \sqrt{E_{seg.1}^2 + E_{seg.2}^2 + \cdots + E_{seg.N}^2} \tag{3}$$

B. Current-Driven Common-Mode Radiation Algorithm

Since the width of a real board is finite, a portion of the magnetic field due to a signal current wraps around the board and there is an effective voltage drop across the return plane. This voltage drop, in turn, can induce common-mode currents that drive various EMI antennas on the board [9]. These EMI antennas could be cables, heatsinks or other metallic structures. At present, three different possible EMI antennas are considered – cable-to-cable, cable-to-board and cable-to-heatsink. Fig. 3 illustrates the cable-to-cable current-driven common-mode radiation mechanism.

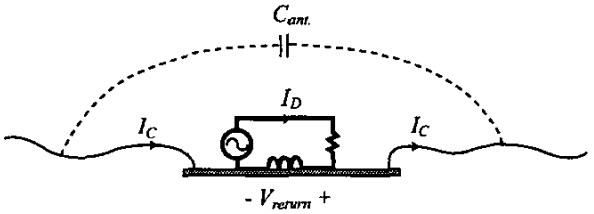

Fig. 3. A simple configuration illustrating current-driven common-mode radiation.

The expert system estimates the voltage difference by approximating the branch inductance of the current return path as [9]

$$L_p = (4/\pi^2)\times\frac{\mu_o\ l\ h}{dist1 + dist2} \tag{4}$$

where, h is the height of the trace over the return plane. $dist1$ and $dist2$ are the two shortest distances to the boundary of the board from the mid point of the segment. The potential difference across the board is calculated as

$$V_{ret} = \omega L_p I_{DM} \tag{5}$$

1) Cable-to-cable algorithm

If there is a pair of cables connected to each end of the board, the potential difference may drive the cables like a dipole antenna. Approximating the antenna as an isotropic radiator, the relation between total radiated power and the voltage across the antenna port is

$$P_{rad} = \oiint \frac{1}{2}\frac{|E|^2}{\eta_o} ds = \frac{2\pi r^2 |E|^2}{\eta_o} \equiv \frac{1}{2} I_C^2\ \ R_{rad} \tag{6}$$

where, η_0=120π. Considering the worst case, the maximum radiation occurs when the EMI antenna resonates. At the resonance frequencies, the input impedance of the antenna is determined by the radiation resistance, R_{rad}, and the common-mode current is

$$I_C = \frac{V_{ret}}{R_{rad}} \tag{7}$$

The default radiation resistance, R_{rad}, used by this algorithm is 100 ohms, which corresponds to the input impedance of a typical worst-case resonant wire antenna [10]. Since the radiated emissions are measured over a conducting plane, the field is multiplied by a factor of two. Finally, plugging (2) into (1) and considering a typical measurement setup, the maximum E field is given by

$$E \approx 2\times\sqrt{\frac{30}{100}}\cdot\frac{V_{ret}}{3} = 0.365\ V_{ret} \tag{8}$$

2) Cable-to-board algorithm

Even if only one cable is connected to the board, it may be driven relative to the board resulting in common-mode current. This algorithm is similar to the *cable-to-cable* algorithm, except that an effective capacitance, C_B, is defined between the cable and the board. The common-mode current is then given as

$$I_C = \frac{V_{ret}}{\sqrt{R_{rad}^2 + 1/(\omega\ C_B)^2}} \tag{9}$$

where the capacitance C_B is approximated as the absolute capacitance of the board and estimated by the equation

$$C_B \approx \varepsilon_o \times \sqrt{Board\ Area} \tag{10}$$

By plugging (9) into (6) and using the same approximations used in the *cable-to-cable* algorithm, the radiated emissions can be calculated as follows,

$$E \approx 0.365 \times \frac{100\ V_{ret}}{\sqrt{100^2 + 1/(\omega\ C_B)^2}} \tag{11}$$

3) Cable-to-heatsink algorithm

This algorithm calculates the radiated field due to common-mode currents on an attached cable driven with respect to a heatsink. The approach is similar to that of *cable-to-board* algorithm but the effective capacitance of the heatsink is used instead of the board. The maximum field strength is given by

$$E \approx 0.365 \times \frac{100\ V_{ret}}{\sqrt{100^2 + 1/(\omega\ C_H)^2}} \tag{12}$$

where C_H is the absolute capacitance of the heatsink.

C. Voltage-Driven Radiation Algorithm

Any metallic structures that are at a different potential than other metallic structures may carry common mode currents and, in turn, create radiated emissions. At this time, the voltage driven radiation algorithm only estimates the radiated fields due to the high-frequency voltages induced on heatsinks in a shielding enclosure. However, it is expected that this algorithm will soon be updated to include the effects of voltages induced on traces, components and other structures with or without a shielding enclosure. The configuration considered in the current algorithm is shown in Fig. 4.

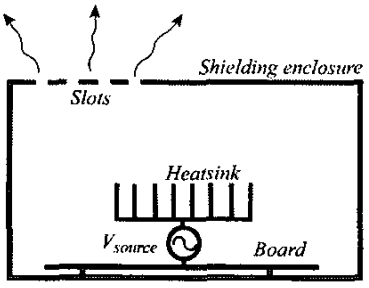

Fig. 4. Radiation due to a heatsink driving enclosure resonances within a shielding enclosure

Although it is difficult to accurately predict the radiated field due to a noise source in a shielding enclosure, an approximate closed-form expression for the radiated emissions from shielding enclosure is available [11]. In this work, the maximum radiated field from a resonant source in a shielding enclosure with small holes or slots is calculated as

$$|E|_{max} = 1.8\times10^{-13} \cdot N\ \ V_s\ \ L^3\ \ f^{1.5}\ \cdot \sqrt{Q/R_s\ \ V} \tag{13}$$

where,

N is the number of slots

L is the slot length

V is the enclosure volume

Q is the Q of the enclosure

V_s is the voltage of the noise source

R_s is the noise source resistance.

All the terms in (13) are expressed in standard mks units.

D. Radiation by I/O Coupling Algorithm

High frequency signals can couple to input/output (I/O) nets that carry the coupled energy away from the board. The common-mode currents induced on the cables attached to I/O nets can result in significant radiated emissions. This emission mechanism is illustrated in Fig. 5.

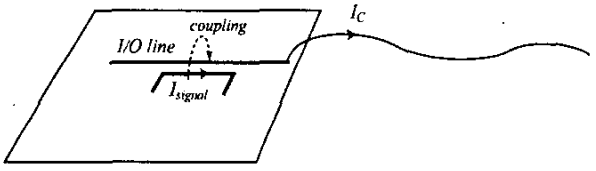

Fig. 5. Common-mode cable current induced by coupling to an I/O trace.

Fig. 5 shows a signal net coupling noise to an I/O net, which then carries the noise off the board. If the signal net and the I/O net are separated by conducting planes, the coupling between the nets is not significant and the algorithm is not applied to these nets. Otherwise, the I/O net is first divided into short segments and the magnitudes of electrically and magnetically coupled signals are calculated.

There are two primary high-frequency trace-to-trace coupling mechanisms, capacitive and inductive coupling. Capacitive and inductive coupling are due to the electric and magnetic fields, respectively. The noise signal voltages induced on I/O lines due to capacitive and inductive coupling are given as

$$V_{elec} = \omega\ \ C_m \times V_{signal} \times l_{eq} \times Z_{rec} \tag{14}$$

$$V_{mag} = \omega\ \ M \times I_{signal} \times l_{eq} \tag{15}$$

where C_m and M are the mutual capacitance and inductance per unit length between two parallel segments [12], [13]. V_{signal} and I_{signal} are the voltage and current on the source segment. l_{eq} is

the equivalent length of a parallel pair of segments and Z_{rec} represents the impedance of the parallel combination of the source and load on the victim net.

The noise voltages induced by both capacitive and inductive coupling are calculated for each I/O net. But, only the maximum value (V_{mag} or V_{elec}) is stored as the noise voltage (V_n) used to estimate emissions. The total noise voltage driving an I/O net is calculated as the sum of the induced noise voltages on each segment of the IO net.

The radiated field strength is calculated in a manner similar to the current-driven algorithm considering the EMI antenna to be an isotropic radiator. The common-mode current is estimated as

$$I_{CM} = \frac{V_n}{Z_{ant}} \tag{16}$$

where Z_{ant} is determined by the configuration of the connector to which the cable is attached. If the connector is shielded, Z_{ant} is assigned a value of 800 Ω. For unshielded connectors, the value of Z_{ant} is the minimum of 800 Ω or 80(N+1) Ω, where N is the number of ground pins in the connector.

Plugging (16) into (6), the estimate of the radiated emissions measured at 3 m over a conducting floor is,

$$E_{rad} = 40 I_{CM} \tag{17}$$

Equation (17) is derived based on the worst-case assumption of an antenna of resonant length. But at low frequencies, attached cables are not likely long enough to resonate in a standard test configuration. At low frequencies, it is more reasonable to calculate the radiated field for an electrically short antenna as [10]

$$R_{rad} = 80\pi^2 \left(\frac{l}{\lambda}\right)^2 = 80\pi^2 \left(\frac{f l}{c}\right)^2 \tag{18}$$

where, l is the length of an antenna and c is free-space wave velocity. A standard configuration for an EMI test is to place the DUT on a table 1 m over a conducting floor. This suggests that the length of cable can be modeled as 1 m with reasonable accuracy. By plugging (18) into (6), the radiated field at low frequencies is estimated as

$$E_{rad} = 3.4\times10^{-7} f I_{CM} \tag{19}$$

Equation (17) and (19) are approximately equal at 118 MHz. Therefore, the radiated field due to the IO coupling mechanism is calculated by using (19) up to 118 MHz and (17) above 118 MHz.

This algorithm considers an I/O net to be any net connected to a connector through any number of series passive devices. For these extended I/O nets, the algorithm calculates the coupled noise voltage on each segment using the algorithm described above. For each extended I/O net, the calculated estimate of the radiated electric field is stored. If the field radiated due to an I/O net is greater than 10 μV/m, the name of the I/O net is stored to report as a possible EMI problem. The total radiation at each frequency is calculated as the root mean square of all the estimates,

$$E_{total} = \sqrt{E_{I/O\,net\,1}^2 + E_{I/O\,net\,2}^2 + \cdots + E_{I/O\,net\,N}^2} \tag{20}$$

III. Analysis Example

There are two commercial EMC expert system tools that use the algorithms described above. One is *Quiet Expert* from Mentor Graphics and the other is *EMC-Engineer* from Zuken. To validate the expert system approach, a "Memory Access Interface" board design was analyzed using *Quiet Expert* Version 4.1.

A. Configuration of the Test Board

The test board is a 4-layer board using CMOS technology. The stack-up of the board is shown in Table I and the layout is shown in Fig. 6. The large number of signal nets in this design makes it difficult to visually identify potential EMC problems.

TABLE I. Table Type Styles

Layer	Material	Thickness	ε_r
Top	Metal Dielectric	1.2 mils 8.0 mils	1.0 4.5
GND	Metal Dielectric	1.2 mils 8.0 mils	1.0 4.5
VDD	Metal Dielectric	1.2 mils 8.0 mils	1.0 4.5
Bottom	Metal	1.2 mils	1.0

B. Analysis Results

Quiet Expert quickly identified two potential problems with the design in Fig. 6. One problem was identified by the *Radiation by I/O Coupling* algorithm and the other was identified by the *Current-Driven Common-Mode* algorithm.

Figure 7a shows part of the Quiet Expert output which indicates that the net called DATA2 couples too strongly with an I/O net. The routing of the DATA2 net is illustrated in Fig. 8. The net is a data line from U4 (a memory controller) to U6 (memory) and U20 (a tri-state transceiver). *Quiet Expert* has identified that this net is coupled to an I/O net called GRESET such that the common mode radiation (VCM_E) is higher than a preset limit. GRESET was identified as an I/O net because it is connected to the outside world via the connector P2. Fig. 7 (a) indicates that the net DATA2 has the potential to induce noise on net GRESET such that the radiated electric field at 3 meters is as much as 27 dBμV/m at a frequency of 130 MHz.

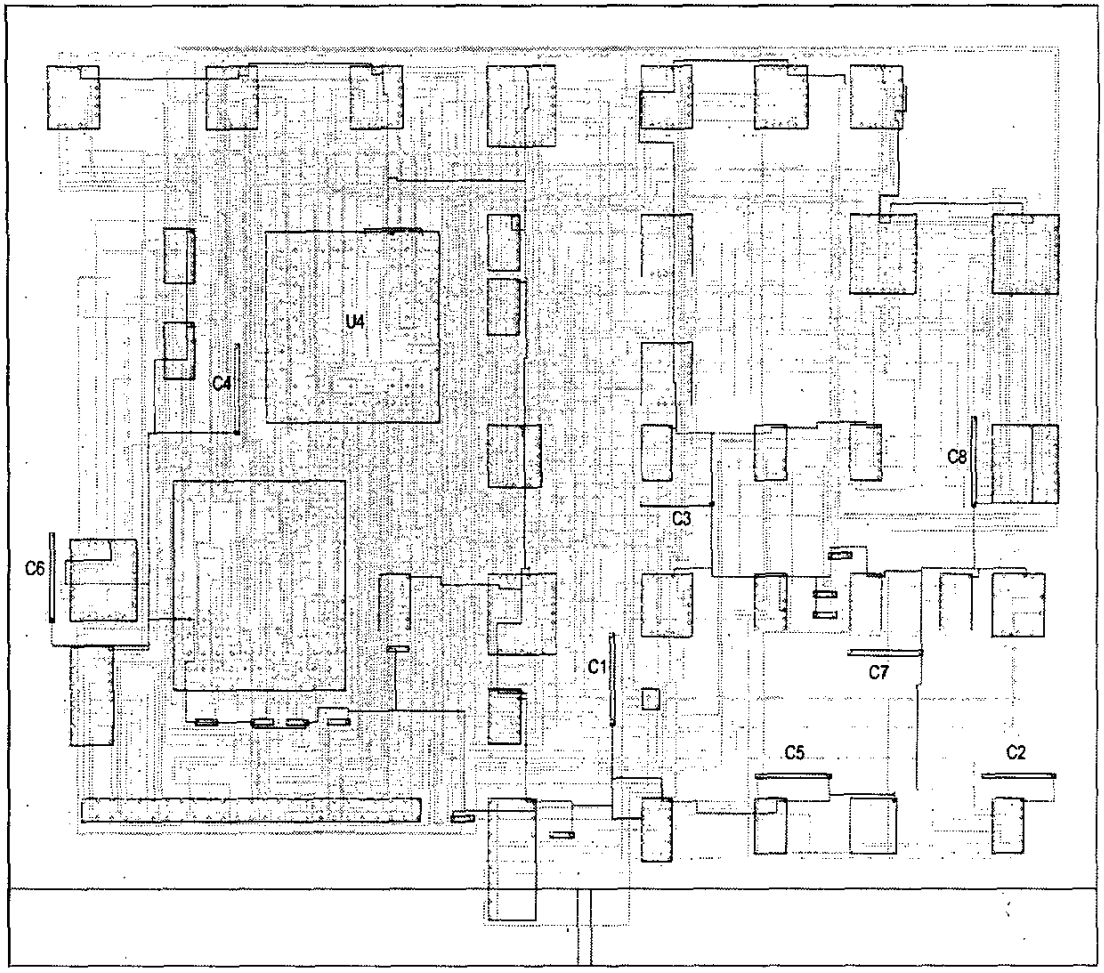

Fig. 6. Layout of the sample board.

Problem: UMR Signal Net Analysis - This net is coupled to I/O Net GRESET.

Advice: Re-Route this net or I/O Net GRESET

DRC	Net	Summary	Total_E/Frequency	DM_E/Frequency	ICM_E/Frequency	VCM_E/Frequency	Antennas
All	All	All	All	All	All	All	All
UMR Signal Net Analysis	DATA2	Edge Rate Too Fast	28.0 450.0	24.0 710.0	19.0 595.0	27.0 130.0	C--B
UMR Signal Net Analysis	DATA2	Coupled to I/O Net	28.0 450.0	24.0 710.0	19.0 595.0	27.0 130.0	C--B
UMR Signal Net Analysis	DATA2	Voltage driven common mode	28.0 450.0	24.0 710.0	19.0 595.0	27.0 130.0	C--B

(a) Predominantly coupling to I/O.

Problem: UMR Signal Net Analysis - The ground noise voltage drives Connector P2 against Connector P1.

Advice: Locate Connector P2 and Connector P1 closer to each other

DRC	Net	Summary	Total_E/Frequency	DM_E/Frequency	ICM_E/Frequency	VCM_E/Frequency	Antennas
All	All	All	All	All	All	All	All
UMR Signal Net Analysis	$1I6\CLKCPU	Current driven common mode	52.0 650.0	50.0 750.0	49.0 450.0	-99.0 50.0	C--C
UMR Signal Net Analysis	$1I6\CLKCPU	Edge Rate Too Fast	52.0 650.0	50.0 750.0	49.0 450.0	-99.0 50.0	C--C
UMR Signal Net Analysis	$1I6\CLKCPU	Too Much Surface Route	52.0 650.0	50.0 750.0	49.0 450.0	-99.0 50.0	C--C

(b) Predominantly current-driven common-mode.

Fig. 7. Results of the test board analysis using Quiet Expert.

As indicated in Fig. 7 (b), Quiet Expert has identified another problem which is even more significant. The net named $1I6\CLKCPU is a significant source of differential mode and current-driven common-mode emissions. The right-most column lists the antenna mechanism responsible for the current driven common mode radiation. In this case it is C-C meaning "connector to connector" or "cable to cable". The net is a clock net driven by the clock driver (U19) and

connected to U1 (a data processing unit) and U37 (an inverter). This clock net produces a voltage drop across the return plane capable of driving significant common-mode currents onto cables connected to connectors P1 and P2. The software estimates a potential current-driven common-mode radiation of 49.0 dBμV/m.

Although both of the layout problems identified by Quiet Expert might have been obvious to an EMC engineer who was familiar with the board and the signals on each of these nets, a lot of effort would have been required to initially locate these problems manually. If changes were made to the layout, this effort would have to be repeated to ensure that no new problems were created. The expert system algorithms are designed to help both experts and non-experts find major potential problems early in the design process without manually examining every net routed on the board.

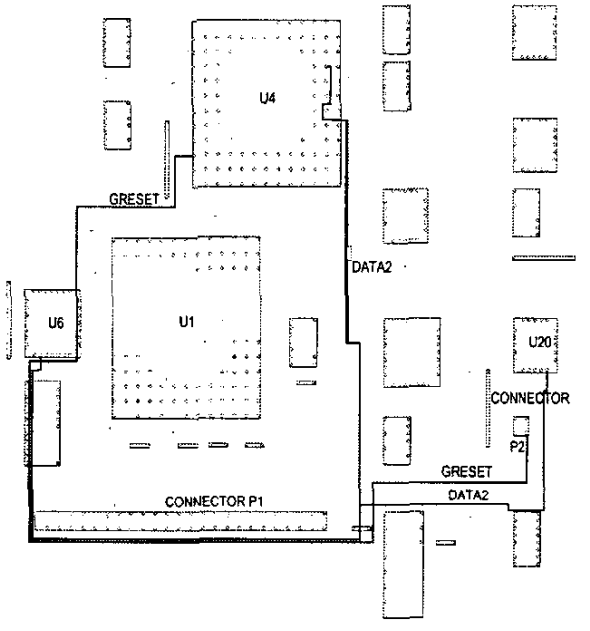

Fig. 8. Layout of DATA2 and GRESET nets

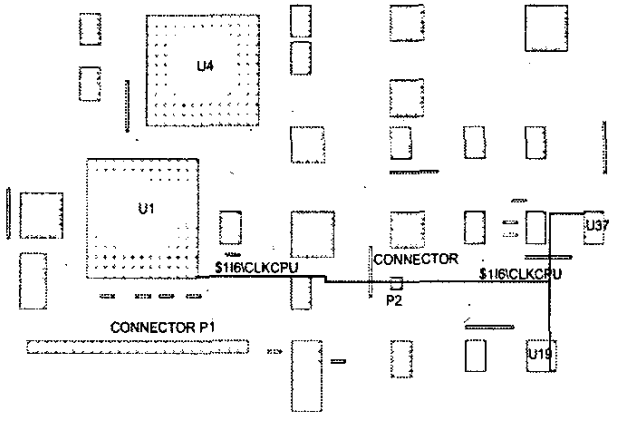

Fig. 9. Layout of the $116\CLKCPU net

IV. Conclusion

Algorithms used to predict possible radiated emissions problems from a printed circuit board have been presented. Four different radiation mechanisms were considered. From an accuracy point of view, this expert system approach is no better than a human EMC expert with a thorough knowledge of the board and a hand calculator. Like a human EMC expert, the algorithms must make assumptions and approximations about how the board will interact with the rest of the system. However, unlike a human expert, the expert system is capable of identifying potential problems with complex board designs in minutes rather than hours or days.

A sample board analysis was presented. The results suggest that software implementing these algorithms identifies the same potential problems that a human EMC expert is likely to identify given enough time.

References

[1] W. B. Halaberda and J. H. Rivers, "Measurement Comparisons of Radiated Test Facilities," Proc. IEEE Int. Symp. on EMC, Anaheim, CA, pp. 401-406, Aug. 1992.

[2] T. Hubing, J. Drewniak, T. Van Doren and N. Kashyap, "An Expert System Approach to EMC Modeling," *Proc. of IEEE Int. Symp. on EMC*, Santa Clara, CA, pp.200-203, Aug. 1996.

[3] N. Kashyap and etc., "An Expert System for Predicting Radiated EMI from PCB's," *Proc. of 1997 IEEE Int. Symp. on EMC*, Austin, Texas, pp.444-449, Aug. 1997.

[4] Joe LoVetri, Suhayya Abu-Hakima, Andrew S. Podgorski, and George I. Costache, "HardSys: Applying Expert System Techniques to Electromagentic Hardening," *Proc. of IEEE Int. Symp. on EMC*, pp.383-385, May 1989.

[5] Joe LoVetri and Andrew S. Podgorski, "Evaluation of HardSys: A Simple EMI Expert System," *Proc. of IEEE Int. Symp. on EMC*, pp.228-232, Aug. 1990.

[6] K. Nageswara Rao, P. Venkara Ramana, M. Krishnamurthy and K Shrinivas, "EMC Analysis in PCB Designs Using An Expert System," *Proc of IEEE Int. Symp. on Electromagnetic Interference and Compatibility*, 6-8 Dec. 1995

[7] Y. Fukumoto, S. Miura, H. Ikeda, T. Nakayama, S. Tanimoto, and H. Uemura, "A Method of Automatic Placement that Reduces Electromagnetic Radiation Noise from Digital Printed Circuit Boards," *Proc. of IEEE Int. Symp. on EMC*, pp.363-368, Aug. 2000.

[8] C. Paul, *Introduction to Electromagnetic Compatibility*, New York: Wiley, 1992.

[9] D. Hockanson, J. Drewniak, T. Hubing, T. Van Doren, F. Sha, and M. Wilhelm "Investigation of Fundamental EMI Source Mechanisms Driving Common-Mode Radiation from Printed Circuit Boards with Attached Cables," *IEEE Trans. Electromag. Compat.*, vol. 28, pp. 557-565, Nov. 1996.

[10] Constantine A. Balanis, *Antenna Theory Analysis and Design*, 2nd ed., 1997.

[11] M. Li, S. Radu, J. Drewniak, T. Hubing, T Van Doren, R. DuBroff, "An EMI Estimate for Shielding Enclosure Design," *Proceedings of the 13th International Zurich Symp. And Technical Exhibition on EMC*, Zurich, Switzerland, pp. 369-374, Feb. 1999.

[12] K. C. Gupta, Ramesh Garg, Inder Bahl, and Prakash Bhartia, *Microstrip Lines and Slotlines*, 2nd edition, Artech House, Norwood, MA, 1996.

[13] Theodore Zeeff, et al., "Microstrip Coupling Algorithm Validation and Modification Based on Measurements and Numerical Modeling," *Proc. of the 1999 IEEE International Symposium on Electromagnetic Compatibility*, Seattle, WA, pp. 323-327, August 1999.